PCCP

Cite this: *Phys. Chem. Chem. Phys.*, 2012, **14**, 3435–3443

www.rsc.org/pccp

PAPER

Unravelling the specific site preference in doping of calcium hydroxyapatite with strontium from *ab initio* investigations and Rietveld analyses

Jacek Zeglinski,*[a] Michael Nolan,[b] Michael Bredol,[c] Andrea Schatte[c] and Syed A. M. Tofail*[a]

Received 6th October 2011, Accepted 19th January 2012
DOI: 10.1039/c2cp23163h

Strontium can be substituted into the calcium sublattice of hydroxyapatite without a solubility limit. However, recent *ab initio* simulations carried out at 0 K report endothermic nature of this process. There is also striking discrepancy between experimentally observed preference of Sr doping at Ca-II sites and the first principles calculations, which indicate that a Ca-I site is preferred energetically for the Sr substitution. In this paper we combine insights from Density Functional Theory simulations and regular configurational entropy calculations to determine the site preference of Sr doping in the range of 0–100 at% at finite temperatures. In addition, samples of Sr–HA are synthesized and refinement of the relevant structural information provides benchmark information on the experimental unit cell parameters of Sr–HA. We find that the contribution of the entropy of mixing can efficiently overcome the endothermic excess energy at a temperature typical of the calcining step in the synthesis route of hydroxyapatite (700–950 °C). We observe that the most preferential substitution pattern is mixed substitution of Sr regardless of the concentration. For a wet chemical method, carried out at a moderate temperature (90 °C), the mixed doping is still slightly favourable at higher Sr-concentrations, except the range at 20% Sr, where Site II substitution is not restricted energetically and equally possible as the mixed doping. We observe a close correspondence between our theoretical results and available experimental data. Hence it should be possible to apply this theory to other divalent dopants in HA, such as Zn^{2+}, Mg^{2+}, Pb^{2+}, Cu^{2+}, Ba^{2+}, Cd^{2+} *etc.*

1. Introduction

Hydroxyapatite (HA) mineral ($Ca_{10}(PO_4)_6(OH)_2$) is a main inorganic constituent of bone and tooth enamel. The synthetic equivalents of the material are used *e.g.* in clinical orthopaedics for spacing or filling bone defects, in femoral plugs in total hip replacement, and HA coating on metal components for cementless fixation.[1] Hydroxyapatite constituting bone is a reservoir of trace ions such as Zn^{2+}, Sr^{2+}, Mn^{2+}, F^{-}, CO_3^{2-}, and SiO_4^{4-}, which play an important role in mediation of biological processes.[2] Strontium ions, for example, decrease bone *resorption* by inhibiting osteoclastic activity and simultaneously promoting bone formation by enhancing pre-osteoblastic cell replication and osteoblastic differentiation.[3] The beneficial action of strontium-doped HA has been recently demonstrated in the *in vitro* experiment on the osteoblast-like cells cultured on the Sr–HA nanocrystals with 3–7 at% Sr.[4] It has been also shown that the Sr–HA material significantly influences the response of primary cultures of rat osteoblasts resulting in higher proliferation and increased values of the differentiation parameters.[5]

It is known that the Sr–HA serves as a reservoir of biologically active Sr ions, being slowly released from the HA surface. However, the biological mechanisms underlying such beneficial effects of strontium are not fully understood so far. The effects of strontium on the osteogenic differentiation of human mesenchymal stem cells (MSCs) were recently studied using a defect model in rats. It was found that strontium could enhance the osteogenic differentiation of the MSCs with upregulated extracellular matrix (ECM) gene expression and activated Wnt/β-catenin pathway.[6] Another *in vivo* work indicates that the Sr treatment profoundly increases osteoprotegerin (OPG) gene expression in the tibias and OPG protein levels in the sera of wild-type mice. This study also concludes that the inhibition of osteoclastogenesis and bone resorption is possibly associated with OPG upregulation by Sr treatment.[7]

The crystal structure of HA can be modified by substitution of foreign ions in both its cationic and anionic sites. Because of

[a] *Materials and Surface Science Institute, University of Limerick, Ireland. E-mail: jacek.zeglinski@ul.ie, jzeglinski@gmail.com, tofail.syed@ul.ie*
[b] *Tyndall National Institute, University College Cork, Cork, Ireland*
[c] *Department of Chemical Engineering, University of Applied Sciences, Münster, Germany*

potentially fruitful applications, a growing interest in synthesis of HA bioceramics containing Sr and other dopants, such as Zn, Mg, Mn, Si, Fe, Eu and La, has been observed in recent years.[8,9] In parallel, a considerable amount of work has been devoted to understand the mechanism of ionic preference and associated changes of the atomic arrangement in the crystal lattice with substitution of strontium.[10–16] In the unit cell of a HA crystal there are ten sites occupied by calcium ions—four of them, denoted Ca-I, form channels parallel to the *c*-axis (Site I), and the remaining six, named Ca-II (Site II), are located around hydroxyl channels and form calcium triangles.

Interestingly, when substituting for Ca, various divalent metal cations show different site preferences, and there is no single mechanism driving the substitution. It has been postulated that smaller ionic radius of Zn compared to Ca is a major factor in accounting for the substantial shrinkage of polyhedron volume when substituting Zn at the Ca Site I positions, which then favours Site II occupancy.[17] Electronegativity is another factor influencing the site preference as it determines the balance between ionic and covalent character of the metal–oxygen bonding. The more covalent character of the metal–hydroxyl oxygen, M–OH bond, accounts for the higher strength of the bonding. This theory is consistent with *e.g.* preferential occupancy of the Ca-II site by Pb and Zn with their electronegativities being, respectively, 2.33, and 1.65, compared to 1.00 for Ca.[10,18] The electronegativity of Sr is close to that of Ca (0.95 *vs.* 1.00) so for this case, it is primarily differences in ionic radii and associated spatial effects that need to be taken into account. As the ionic radius of Sr^{2+} is bigger than that of Ca^{2+} (0.112 nm *vs.* 0.099 nm), it can be expected that the crystal lattice of HA will expand with the substitution of Ca^{2+} with Sr^{2+}. In fact, structural characterizations of Sr-doped HA performed with X-ray diffraction data and Rietveld refinement have shown a linear expansion of the unit cell of HA and no miscibility limit has been observed for the range of substitutions from 0 to 100% of Sr.[10,11,13]

Structural refinement of Sr–HA by a Rietveld method has recently been published. Bigi *et al.* have reported a preference for the Site II substitution at or above 10 at% of Sr, while Site I was preferred at 5 at%.[11] According to independent works of Zhu *et al.*[10] and O'Donnell *et al.*,[13] a preferential Sr occupancy at Site II has been observed for HA in the range of *ca.* 20–80 at% of the dopant, being the most pronounced from 50 to 80 at% as reported by Zhu *et al.* Terra *et al.* combined first-principles modelling and XRD refinement to investigate systems with up to 20 at% of Sr.[15] Their results of Rietveld refinement showed that Sr occupies Site I at the concentration below 1 at%. The ideal statistical occupancy ratio has been, however, observed for systems containing 5 at% Sr, contrary to the work of Bigi *et al.* The highest investigated concentration of Sr in ref. 15 was 15 at% and here a slight preference for the Site II substitution was found. Terra *et al.* also performed *ab initio* investigation of the energetic preference for Sr substitution at non-equivalent Ca-I and Ca-II sites for a simulated supercell containing 0–20 at% Sr in solid solutions of HA. The authors found that at 0 K strontium prefers the Ca-I site. Matsunaga and Murata used first-principles methods to study the Sr site preference in the whole range of substitution, from 0–100 at%.[16] They also observed the energetic preference for doping Sr at Site I, regardless of the concentration. The energy computed in both the *ab initio* works was calculated based on relaxation of atomic positions within simulated lattice, while the unit cell parameters (size and shape) were not allowed to relax, but held fixed. It is clear that there is no universal agreement in terms of the preferred Sr occupancy in Ca-I and Ca-II sites of HA among experimental reports available. An even more striking discrepancy appears when comparing experimental and theoretical results.

It is now important to combine the theoretical study that approaches the experimental reality more closely. Here we combine insights from *ab initio* simulations, with relaxed atomic positions and unit cell parameters and regular configurational entropy calculations to determine the specific site preference of Sr substitution in HA in the range of 0–100 at% at finite temperatures. The simulated crystal structures are fully-optimized allowing for the relaxation of atomic positions and the unit cell volume. In this way even subtle changes in the crystal cell dimensions can be tracked as a function of dopant concentration. According to our knowledge such an approach has not been applied to the investigated system so far. Three theoretical sequences of doping are considered: (i) preferential substitution of Sr in Site II, (ii) preferential substitution of Sr in Site I, and (iii) mixed substitution. In addition, polycrystalline HA samples containing 0–100 at% Sr are synthesized by means of a solid-state route and the relevant X-ray data are refined by the Rietveld method, providing a benchmark information on the experimental unit cell parameters of Sr–HA.

2. Materials and methods

2.1. Experimental part

A solid-state method is used to synthesise Sr-doped hydroxyapatite ($Ca_{(10-x)}Sr_x(PO_4)_6(OH)_2$) with Sr concentrations at 0, 10, 25, 50, 75 and 100 at%. The procedure of preparing 3 g of 50% Sr-doped HA powder ($Ca_5Sr_5(PO_4)_6(OH)_2$) is described briefly: 2.213 g of strontium hydroxide (Sigma-Aldrich, purity 95%), 0.191 g of calcium hydroxide (Sigma-Aldrich, purity 95%), and 2.385 g of diammonium hydrogen phosphate (Sigma-Aldrich, purity 99.2%) were mixed with 30 mL of distilled water and 50 g of zirconia balls (3 mm in diameter). The mixture was initially homogenised in an ultrasonic bath for 2 h at 65 °C and then milled in a ball-mill for 6 h at a rotation speed of 56 rpm. The powders were sieved, dried in an oven for 12 h at 85 °C and calcined for 3 h at 950 °C.

The structural analysis of Sr-substituted HA was carried out with a PANalytical X'pert PRO-MPD diffractometer. The X-ray diffraction patterns were recorded with Cu Kα radiation in the 2Θ range of 20–60° at the step size of 0.008°/2Θ and the scan speed of 0.02° s^{-1}. The X-ray power used was 40 kV with a filament current of 35 mA. To obtain statistically-relevant data, the sample holder was allowed to rotate at a spinning speed of 15 rpm. The Reflex software (Accelrys) was used to refine crystal structures of the samples in the 2Θ range of 20–60° by the Rietveld method.

2.2. Theoretical model and computational details

An atomistic model of the hydroxyapatite crystal is constructed based on hexagonal $P6_3$ symmetry and experimental values of

the single crystal lattices of HA refined by Sudarsanan and Young ($a = b = 9.424$ Å, $c = 6.879$ Å, $\alpha = \beta = 90.00°$, $\gamma = 120.00°$).[19] The unit cell of HA contains 10 Ca ions. This indicates that there are potentially 10 positions to be occupied by strontium, with four Ca-I sites located in calcium columns and six Ca-II sites positioned around the OH groups. Models of Sr-doped HA are built by a progressive substitution of Ca by Sr at a 10 at% interval, ranging from 0% to 100% Sr–HA. Three theoretical sequences of Sr-doping are considered in this work:

1. First 6 Sr atoms are substituted into Ca-II sites, then 4 Sr into the Ca-I sites.

2. First four Sr atoms are substituted into Ca-I sites followed by a substitution of 6 Sr into the remaining Ca-II sites.

3. Mixed substitution of strontium starting from Ca-II sites.

All calculations are carried out in the periodic plane wave approach using density functional theory (DFT) in the VASP code (v. 5.2),[20–22] in which valence electronic states are expanded in a set of periodic plane waves and the interaction between the core and the valence states is treated with the projector augmented wave (PAW) method.[23,24] We use the PW91 GGA exchange–correlation functional,[25] a 450 eV plane wave cut-off energy, and Monkhorst–Pack grids with a $4 \times 4 \times 4$ k-points mesh to perform the Brillouin zone integrations for both the geometry and energy calculations. The optimisation is performed in two steps. In the first step atomic positions are optimised in a fixed unit cell; in the second step both atoms and lattice constants are allowed to relax. Changes in total energy as a function of Sr substitution in HA are calculated as excess energy (E_x^{E}) of the solid solution $Sr_xCa_{1-x}HA$ relative to those of the two end members CaHA and SrHA, with 100% Ca and 100% Sr, respectively:

$$E_x^{\mathrm{E}} = E(\mathrm{Ca}_{1-x}\mathrm{Sr}_x\mathrm{HA}) - xE(\mathrm{SrHA}) - (1-x)E(\mathrm{CaHA}) \quad (1)$$

where x is in the range from 0 to 1. Relaxation of all ionic positions is allowed until forces smaller than 0.01 eV Å^{-1} are achieved.

To calculate the influence of temperature on the mixing properties, the substitution of Ca with Sr in the Ca-sublattice of HA was assumed to yield regular solutions, *i.e.* systems, in which the free energy of mixing, ΔF_{mix}, can be decomposed into an excess energy of mixing, E_x^{E}, and an ideal entropy of mixing, and y_i being the proper molar fractions of Ca and Sr:

$$\Delta S_{\mathrm{mix(id)}} = -nR\,\Sigma(y_i \ln(y_i)) \quad (2)$$

The free energy of mixing is thus calculated as follows:

$$\Delta F_{\mathrm{mix}} = E_x^{\mathrm{E}} - T\Delta S_{\mathrm{mix(id)}} \quad (3)$$

In a unit cell with 10 Ca-sites (one "mol"), there are three limiting possibilities to form solid solutions:

(1) Random mixing over Ca-I and Ca-II sites (seq. 3): all sites are available for mixing ($n = 10$), and the compositional parameter y in the equation for $\Delta S_{\mathrm{mix(id)}}$ is identical to the molar fractions x_i of Sr and Ca in the unit cell.

(2) Preferred substitution in Ca-II sites (seq. 1): first all 6 Ca-II sites are filled, and the associated ideal entropy gain is calculated with $n = 6$ (available sites for mixing) and a compositional parameter y for $\Delta S_{\mathrm{mix(id)}}$, which is rescaled by $y = x/0.6$. At $x = 0.6$, Ca-II would be fully substituted, thus no mixing entropy gain can be expected any more. At still higher x-values, the associated ideal entropy gain is calculated with $n = 4$ (available sites for mixing) and a compositional parameter y for $\Delta S_{\mathrm{mix(id)}}$, which is now rescaled by $y = (x - 0.6)/0.4$.

(3) Preferred substitution in Ca-I sites (seq. 2): first all 4 Ca-I sites are filled, and the associated ideal entropy gain is calculated with $n = 4$ (available sites for mixing) and a compositional parameter y for $\Delta S_{\mathrm{mix(id)}}$, which is rescaled by $y = x/0.4$. At $x = 0.4$, Ca-I would be fully substituted, thus no mixing entropy gain can be expected any more. At still higher x-values, the associated ideal entropy gain is calculated with $n = 6$ (available sites for mixing) and a compositional parameter y for $\Delta S_{\mathrm{mix(id)}}$, which is now rescaled by $y = (x - 0.4)/0.6$.

With this approach, T-dependent free energies of mixing have been calculated in order to identify the thermodynamic driving forces for mixing. The choice of temperature is somewhat arbitrary, since it depends on the cooling procedure from equilibration at 950 °C down to a fictive temperature that finally is frozen in. We can safely assume that below 3/4 of the equilibration temperature, mobility of ions is becoming so small that no further equilibration will take place any more.

3. Results and discussion

3.1 Experimental unit cell of Sr-doped HA

The X-ray diffraction patterns of $Ca_{(10-x)}Sr_x(PO_4)_6(OH)_2$ with Sr concentrations at 0, 10, 25, 50, 75 and 100 at% confirmed the presence of single-phase, crystalline materials. The β-TCP phase was not observed in our Sr-doped HA samples. The patterns of Sr-doped HA were similar to that of pure HA, but a slight systematic shift of all peaks to lower 2θ angles with the substitution has been observed, indicating expansion of the crystal lattice. Table 1 collates experimental parameters a and c of the Sr-doped HA crystals from our work and available literature data refined using the Rietveld method. Fig. 1 shows an example Rietveld fit to the XRD pattern of our sample consisting of 50% Sr–HA.

A very good agreement can be seen between the refinement results from our samples, synthesized by a solid-state method, and single-crystal data for undoped HA,[19] and 100% Sr–HA,[26] obtained by Sudarsanan and Young and also those from the powder refinements reported by other groups.[11,13,15] Our results confirm that the unit cell of hydroxyapatite expands linearly with strontium doping in the range of 0–100 at%. This relationship can be described with the following equations of linear fit: $a = 0.0033x + 9.4232$; $R^2 = 0.994$, and $c = 0.004x + 6.8829$; $R^2 = 0.997$.

3.2 *Ab initio* simulations

Crystal structure of $Ca_{1-x}Sr_xHA$. In the present work we study three theoretical sequences of Sr doping in HA. In the first step of doping (seq. 1), a single Sr atom replaces one Ca-II atom located at the edge of the unit cell, yielding a cell with 10 at% Sr. In the next steps, second and subsequent four Sr atoms replace Ca in Ca-II sites. The remaining four Ca-I sites are filled by Sr, ending with full substitution and the formation

Table 1 Comparison of lattice parameters of Sr-doped HA from Rietveld-refined experimental X-ray diffraction data

Sr at. (%)	0	10	25	50	75	100
a/Å	9.4224 (1)[a]	9.4494 (1)[a]	9.5119 (1)[a]	9.5908 (2)[a]	9.6898 (2)[a]	9.7450 (9)[a]
	—	9.451[b]	—	9.603[b]	—	—
	—	9.471[c]	—	—	—	—
	9.411[d]	—	9.505[d]	9.596[d]	9.659[d]	9.777[d]
	9.424[e]	—	—	—	—	9.745[f]
c/Å	6.8834 (1)[a]	6.9171 (2)[a]	6.9828 (2)[a]	7.0826 (3)[a]	7.1950 (3)[a]	7.2688 (2)[a]
	—	6.902[b]	—	7.103[b]	—	
	—	6.923[c]	—	—	—	
	6.877[d]	—	6.950[d]	7.054[d]	7.182[d]	7.288[d]
	6.879[e]	—	—	—	—	7.265[f]

[a] Powder refinement—this work; numbers in parentheses denote standard deviations from Rietveld analyses of the least-significant digit. [b] Powder refinement.[11] [c] Powder refinement.[15] [d] Powder refinement.[13] [e] Single crystal refinement.[19] [f] Single crystal refinement.[26]

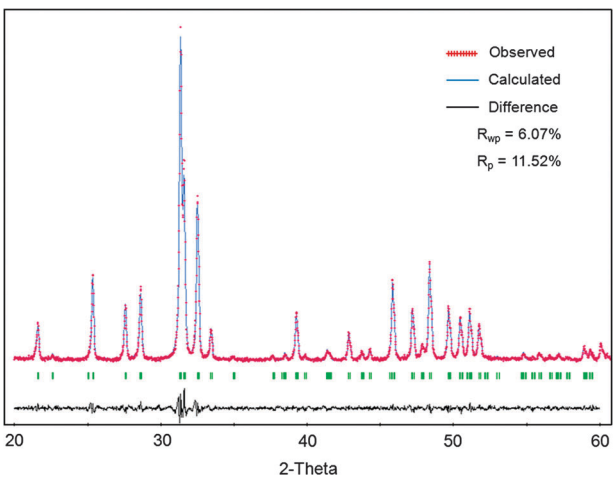

Fig. 1 Rietveld fit to experimental X-ray diffraction pattern of 50% Sr–HA.

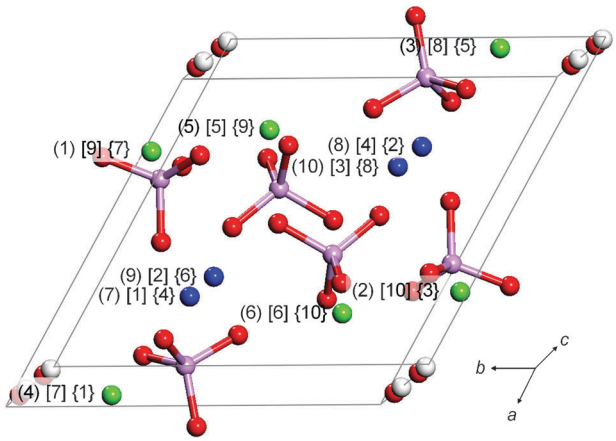

Fig. 2 Atomistic model of a hydroxyapatite unit cell. Atoms of calcium are numbered from 1 to 10 according to the investigated theoretical orders of Sr substitution. Sequence 1: (1), (2),...(10); sequence 2: [1], [2],...[10]; sequence 3: {1}, {2},...{10}. Ca-I—blue, Ca-II—green, O—red, P—purple, H—white.

of Sr–hydroxyapatite. Detailed order of substitution is presented in Fig. 2.

Our calculated unit cell parameters for the undoped HA and 100% Sr-doped HA crystal are: $a = b = 9.494$ Å and $c = 6.887$ Å, and $a = b = 9.842$ Å and $c = 7.321$ Å, respectively, being slightly overestimated compared to those from the experimental XRD refinements (see Table 1). All the optimised structures match the crystal symmetry of HA, regardless of the Sr content, with average values for $\alpha = 90.00° \pm 0.03°$, $\beta = 89.99° \pm 0.05°$, and $\gamma = 120.13° \pm 0.21°$. The lattice constants of HA elongate with increasing concentration of Sr, as it can be expected based on the higher ionic radius of Sr.

Fig. 3 shows changes in volume of the HA unit cell as a function of Sr substitution for the three theoretical sequences considered. Experimental benchmark from our Rietveld refined XRD data is also shown. An excess in the calculated unit cell volume of *ca.* 9 Å^3 (1.7%) is observed in the range of 0–75% Sr compared to the experimental data; the overestimation of the volume is typical of the DFT approach used. The calculated lattice constants and hence the volume are slightly larger, as a result of overestimation by GGA of binding between ions. Nevertheless, the slopes of the theoretical volumes match the experimental one and thus validate our computational approach. As it can be seen from Fig. 4, the lattice dimensions

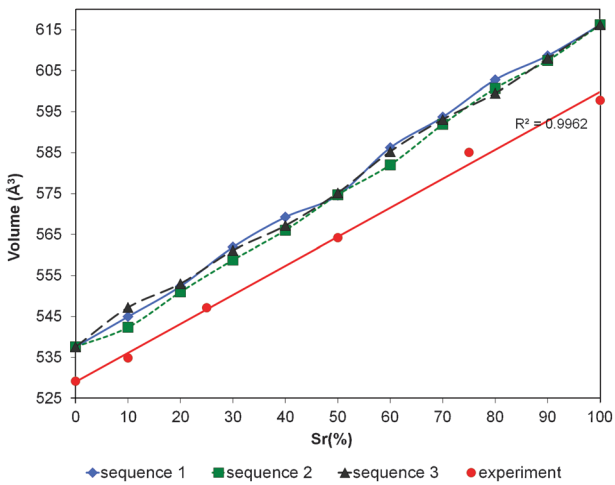

Fig. 3 Theoretical *vs.* experimental changes in volume of the HA unit cell as a function of Sr substitution. Seq. 1: 6 Sr at Site II + 4 Sr at Site I, seq. 2: 4 Sr at Site I + 6 Sr at Site II, seq. 3: mixed substitution.

for the same Sr concentration vary slightly with the Site II to Site I occupancy ratio. The smallest expansion of the unit cell is observed when Sr is doped initially in the Site I positions (seq. 2).

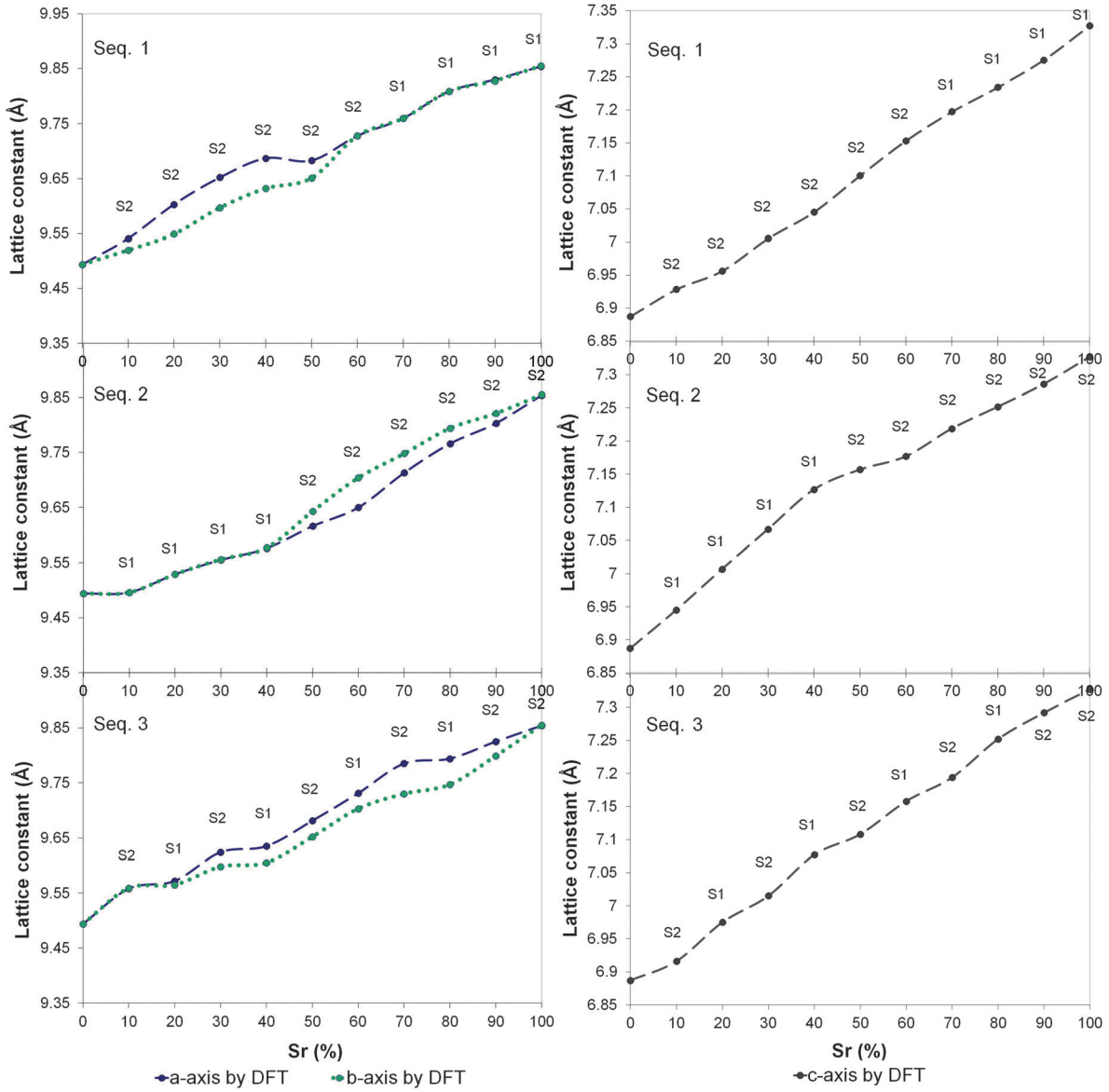

Fig. 4 Calculated changes in *a* and *b* lattice constants (left column), and *c* (right column) of HA for three theoretical sequences of Sr substitution. S1—strontium substituted in Ca-I sites, S2—strontium substituted in Ca-II sites.

As the simulated crystal structures are fully optimized, hence both atomic relocations and the related changes in the crystal lattice can be tracked when doping the unit cell with ions of different volumes. It has been already mentioned that the ionic radius of strontium is bigger than that of calcium (0.112 nm *vs*. 0.099 nm), and we observe expansion of the crystal unit cell of Sr-doped HA both theoretically and experimentally. It is known that for the end members, 100% HA and 100% Sr–HA, the apatite crystal symmetry is not compromised.[19,26] However, for their intermediates, $Ca_{1-x}Sr_xHA$, certain distortions of the HA unit cell can be theoretically expected, resulting in lowering of the crystal symmetry. In fact, we observe that *a* and *b* parameters in our simulated systems do not expand uniformly with the substitution (Fig. 4).

This difference is most pronounced for the initial stages of substitution from 10% to 50% of Sr doping in Ca-II sites (seq. 1); the *a*-axis expands here up to 0.055 Å more than the *b*-axis. In the systems containing 50–90% of Sr doped in Ca-II sites (seq. 2), the expansion of the *b*-axis is more pronounced than the *a*-axis. For mixed substitution (sequence 3), the *a*-axis expands more than *b* in the range of 20–90 at% of Sr in HA. On the other hand a uniform expansion of *a* and *b* lattices can be observed for both the sequences 1 and 2, when Sr is progressively doped into Site I. It can be thus concluded that the progressive doping of Sr into Ca-II sites causes greater expansion and distortion of the crystal structure of hydroxyapatite than its initial systematic substitution into Ca-I sites.

To understand this phenomenon we have examined the effect of the Site I/Site II substitution on the atomic arrangement in a $Ca_{0.6}Sr_{0.4}HA$ system (40 at% Sr); at this Sr concentration we observe pronounced differences in values of the *a* and *b* constants for the doping at Site II, contrary to equal expansion of the *a* and *b* values at the Site I. Fig. 5 compares two supercells of the $Ca_{0.6}Sr_{0.4}HA$, with four Sr atoms doped at Ca-II sites (Fig. 5a)

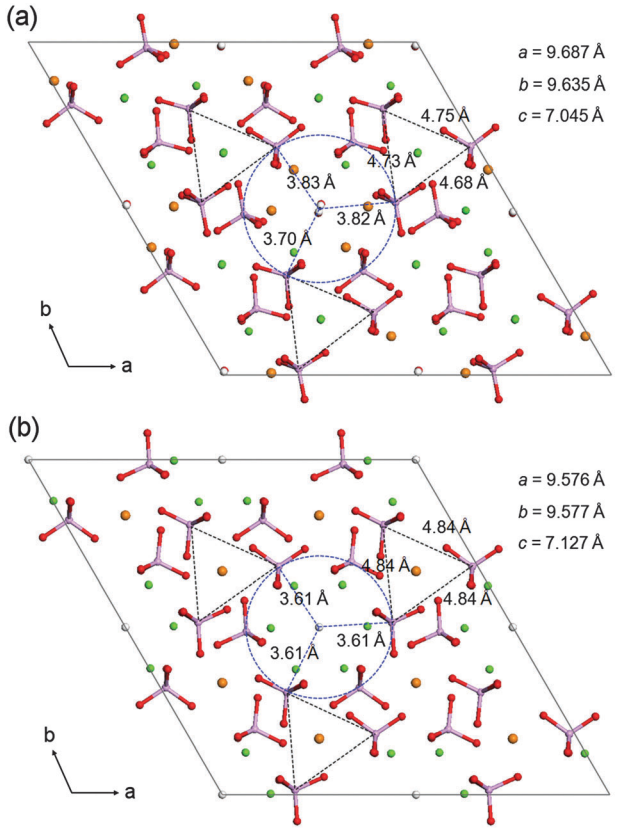

Fig. 5 Crystal structure of $Ca_{0.6}Sr_{0.4}HA$—top view along the *c*-axis. (a) Sr doped at Site II; (b) Sr doped at Site I. Ca—green, Sr—orange, O—red, P—purple, H—white.

versus four Sr doped at Ca-I sites (Fig. 5b). The *c*-axis view shows more uniform distribution of Sr in the crystal lattice when the Site I is being occupied by the dopant (Fig. 5b). In the Site I every metal cation lies between two layers of three phosphate ions. The distances between centres of the PO_4 units are shown as sides of triangles. In the Site II-doped structure (Fig. 5a), the PO_4 are at an irregular distance of 4.68–4.75 Å. Meantime the Sr doping at the Site I imposes a uniform expansion of the PO_4 triangles up to 4.84 Å. This is in good agreement with results of Terra *et al.*, where more local distortions of Site II than Site I was observed with Sr doping, as computed for a fixed unit cell up to 20 at%.[15]

The supercells are centred at a hydroxyl channel with every hydroxyl ion surrounded by three PO_4 units; the radii of the circles drawn in Fig. 5 determine the distances between PO_4 and OH ions. An irregular space of 3.70–3.83 Å is created when Sr is doped onto Ca-II sites and the hydroxyls are slightly slid away from the *c*-axis when interacting directly with Sr^{2+}. On the contrary, the PO_4 tetrahedra are uniformly shifted towards hydroxyl channels as a result of doping at Site I (OH...PO_4 = 3.61 Å).

Based on these observations it can be concluded that Ca-I sites allow for better accommodation of bigger ions such as Sr, as compared to Ca-II sites. This is possible through a uniform shift of the PO_4 tetrahedra, surrounding Sr at the Ca-I sites, towards neighbouring hydroxyl channels. As a result, the crystal lattice expands less in the *a* and *b* direction compared to the Site II substitution. However, the close proximity of the dopants in the *c*-axis oriented Ca-I channels (Sr...Sr = 3.57 Å) results in bigger expansion of the *c*-axis as seen in Fig. 4 (seq. 2).

Free energy of mixing. Fig. 6 shows the calculated excess energy of the solid solution, $Ca_{10-x}Sr_xHA$, for the three theoretical sequences and the related free energy of mixing at three processing temperatures: (i) equilibration temperature, T_{calc} = 950 °C, typical for the annealing/calcination step for HA synthesis by a solid-state method, (ii) the approx. fictive temperature, T_{fict} = 700 °C, and (iii) the temperature at which the wet-chemical synthesis of HA is usually carried out,[15,27] T_{wet} = 90 °C.

All the relative values of excess energy are positive compared to the undoped HA, indicating endothermic nature of the substitution. From comparison of the discussed sequences (Fig. 6a) it appears that the gradual doping of strontium into Ca-I sites is less energetically demanding and thus should be preferential over the doping into Ca-II sites in the range of 20 to 80 at%. The preference for the mixed substitution locates between these two. This, however, relates to 0 K and do not include a stabilizing free energy term, $-T\Delta S$, provided by the entropy of mixing at finite temperature. The Excess Energies from this work are consistent with those of Terra *et al.*[15] and

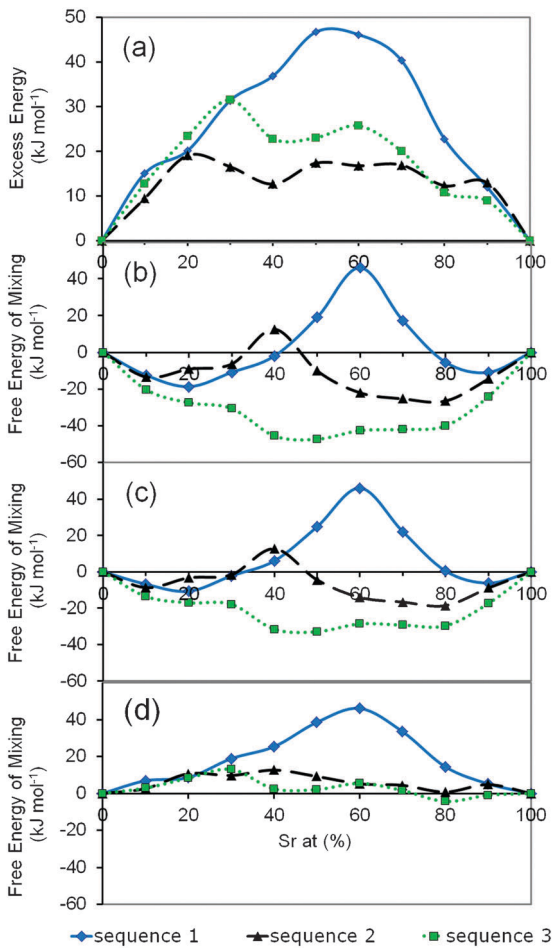

Fig. 6 Calculated excess energy (a) and free energy of mixing at (b) 950 °C, (c) 700 °C, and (d) 90 °C, as a function of Sr substitution in the HA unit cell. Seq. 1: 6 Sr at Site II + 4 Sr at Site I, seq. 2: 4 Sr at Site I + 6 Sr at Site II, seq. 3: mixed substitution.

Table 2 Fractional (%) occupancies of Sr at Site I and Site II from Rietveld refinements

	Fractional (%) occupancy of Sr						
Composition/location	$Ca_{9.9}Sr_{0.1}HA$[a]	$Ca_{9.5}Sr_{0.5}HA$[a]	$Ca_{9.0}Sr_{1.0}HA$[a]	$Ca_{8.5}Sr_{1.5}HA$[a]	$Ca_{7.5}Sr_{2.5}HA$[b]	$Ca_{5.0}Sr_{5.0}HA$[b]	$Ca_{2.5}Sr_{7.5}HA$[b]
Site I	1.9	4.0	9.0	12.0	19.0	48.0	69.0
Site II	0.1	4.0	10.0	16.0	25.0	55.0	80.0
Site II/Site I	0.05	1.00	1.11	1.33	1.32	1.15	1.16

[a] Terra *et al.*[15] [b] O'Donnell *et al.*[13]

Matsunaga and Murata,[16] where a similar Site I preference for the doping at 0 K has been observed.

To calculate the influence of temperature on the site preference of Sr doping in the HA lattice, we assume that the substitutions of Sr in the Ca-sublattice of HA yield regular solutions, *i.e.* systems in which the free energy of mixing can be decomposed into an excess energy of mixing and Entropy of mixing (for the computational details refer to Section 2.2). The free energy of mixing is plotted as a function of Sr doping concentration at T_{calc} = 950 °C (Fig. 6b), T_{fict} = 700 °C (Fig. 6c), and T_{wet} = 90 °C (Fig. 6d). Now it can be seen that the contribution of the entropy of mixing can efficiently overcome the unfavourable excess energy, providing certain processing temperature.

If we consider the temperature typical of the calcining step in the synthesis route we observe that the most preferential substitution pattern is mixed substitution of Sr according to seq. 3 (Fig. 6b and c). Considering the temperature at which low-temperature wet chemical synthesis is carried out (90 °C), the contribution of the Entropy of mixing to the stabilisation of the system is smaller but still sufficient to neutralise the endothermic nature of the Sr substitution at least in seq. 3 at high Sr-concentrations. As for the high-temperature process, for the wet chemical method, the mixed doping is slightly favourable, except the concentrations at around 20 Sr%, where Site II substitution is not restricted energetically and equally possible as the mixed doping (Fig. 6d).

Experiment *vs.* theory. Table 2 collates Rietveld refined fractional occupancies of Sr at Site I and Site II in the range of 1–75 at% in HA from samples synthesised by a wet chemical method.[13,15]

The ratio of Site II to Site I is shown in the table in order to quantify excess of substitution at a site. When the ratio equals 1, this means that the ideal statistical (mixed) occupancy has been achieved and there is no preference in doping either into Site I or Site II. As it can be seen, at a very low amount of Sr (1 at%), there is clear preference of doping at Site I, while at a 5 at% the statistical occupancy ratio is observed. For higher amounts of Sr in the crystal lattice, there is a slight preference of Site II substitution. The highest Site II/Site I ratio of 1.33 and 1.32 has been recorded for the doping at 15 and 25 at%, respectively. At 50 at% and 75 at% the ratio is 1.15 and 1.16, respectively, indicating a prevailing mixed substitution. This experimentally observed site preferences for Sr correspond with our calculated free energies of mixing, regardless of the equilibrating temperature. The differences in the free energy for the three sequences at 20 at% are very small so the doping at Site II is much more probable than at higher Sr concentrations, where energy barrier is expected for the Site II substitution at 50–70 at%, and mixed substitution is more preferential. The computational approach proposed in this work provides a substantial advance compared with previous theoretical works on the site preference of Sr in HA at 0 K. The close correspondence between the experiment and theory shows the applicability of our approach and it should be possible to apply the theory to other divalent dopants substituted in HA, such as Mg^{2+}, Pb^{2+}, Cu^{2+}, Ba^{2+}, Cd^{2+}, Hg^{2+} and Eu^{2+}. In principle the theory could be also applicable to other mechanisms of dopant incorporation, such as recently reported interstitial insertion of zinc ions into hydroxyl channels of the HA crystal.[28] In this particular case the number of interstitial sites to be potentially occupied by Zn in the HA unit cell must be defined, and the equations of the excess energy (eqn (1)) and the ideal Entropy of mixing (eqn (2)) modified accordingly.

Structure and stability of $Ca_{5.0}Sr_{5.0}HA$. It has been shown in our calculations that the Site I/Site II occupancy ratio of Sr influences the energetic stability of the HA crystal structure. As the highest differences in excess energy are observed for the structures containing 50 at% Sr, we thus decided to study various distributions of Sr in Ca-I and Ca-II sites at this concentration. Table 3 presents calculated lattice parameters, unit cell volumes, and relative stabilities at 0 K for the 50% Sr-doped HA at various distributions of strontium in Ca-I and Ca-II sites.

The least stable appears the system **1**, where all five Sr atoms are doped into Ca-II sites. The most stable energetically is the system **3**, where two Sr are located at Ca-I and three Sr at Ca-II sites; this is in fact the ideal mixture with the fractional occupancy ratio Sr2/Sr1 = 1. Systems **4** and **5**, with the higher content of Ca-I site occupancy, are also energetically favourable, with a difference of less than 3 kJ mol^{-1} to the lowest energy structure **3**.

Fig. 7 presents the most stable structural models of 50% Sr–HA (systems **3**, **4**, and **5**). As it can be seen, the different

Table 3 Distribution of strontium in Site I and Site II in 50% Sr-doped HA calculated by DFT. Associated changes in cell volume are shown along with relative stabilities of the systems (ΔE^*)

System name	x Sr in Site I, y Sr in Site II	Volume/Å^3	ΔE^*[a]/kJ mol^{-1}
1	$x = 0, y = 5$	575.7	30.5
2	$x = 1, y = 4$	577.5	10.1
3	$x = 2, y = 3$	572.5	0.0
4	$x = 3, y = 2$	575.6	2.6
5	$x = 4, y = 1$	574.7	2.1
Experiment[b]	—	564.3	—

[a] ΔE^* are given relative to the lowest energy structure **3**. [b] Rietveld refined volume—this work.

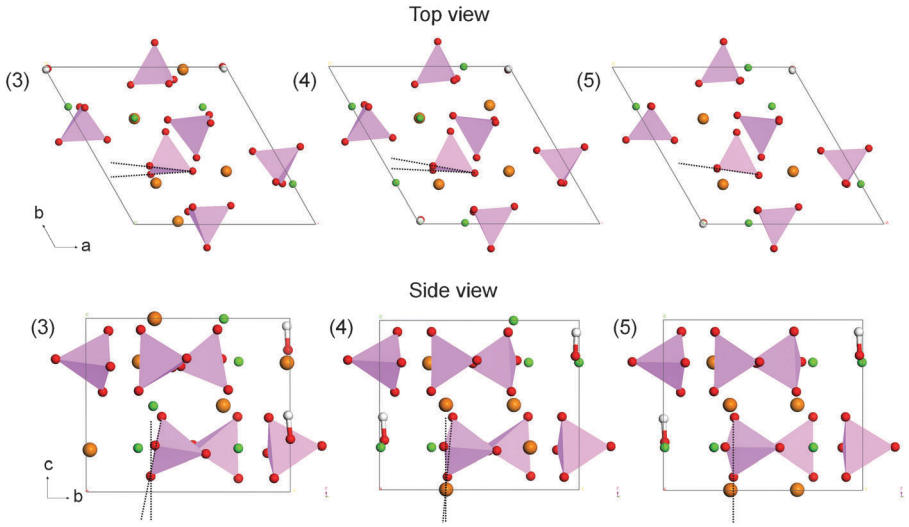

Fig. 7 The most stable energetically structural models of 50% Sr–HA with varying ratios of strontium dopant in Ca-I/Ca-II sites: 2 Sr-I to 3 Sr-II (**3**), 3 Sr-I to 2 Sr-II (**4**), 4 Sr-I to 1 Sr-II (**5**). Ca—green, Sr—orange, O—red, PO_4 tetrahedron—purple, H—white.

arrangement of Sr atoms in the lattice of HA implies certain changes in the positions of surrounding ions. Hydroxyl ions are slightly forced out from their *c*-axes, but still parallel to them. All the six phosphate (PO_4^{3-}) ions preserve their tetrahedral geometry after the substitution, with the average P–O bond length distance of 1.559 ± 0.004 Å, but they are tilted and rotated from their initial positions defined by hexagonal symmetry of the HA crystal. The most prominent changes can be observed for the structure **3**, possessing the lowest ground-state energy; here, the phosphate tetrahedra are more tilted. Meanwhile, a gradual improvement of the crystal symmetry is observed when more Sr atoms occupy Ca-I sites (structure **4** and **5**), with the structure **5** presenting nearly undistorted arrangement of PO_4 tetrahedra. Thus, certain distributions of strontium in the HA lattice impose a perturbation of the structural arrangement and lower crystal symmetry. A substantial difference from a crystallographic point of view is the absence of a center of symmetry in the certain Sr-doped, lower symmetry structures as compared to the centro-symmetric hexagonal $P6_3$ or monoclinic $P2_1/b$ crystal systems of hydroxyapatite. Similar phenomenon has been observed by Haverty *et al.*,[29] for undoped synthetic HA. The authors have observed comparable distortions of phosphate tetrahedra in the DFT-optimised structure of undoped HA and a good match of the model and the Rietveld-refined experimental XRD pattern. Based on that, they have postulated the presence of a non-centro-symmetric lower symmetry phase, monoclinic $P2_1$, in the synthetic HA crystal. It could be now speculated that the theoretically predicted phosphate tetrahedral rotation, as can be observed *e.g.* in the structure **3**, resulting in the absence of a center of symmetry, could potentially enhance the peculiar dielectric properties of apatite such as pyroelectric surface charge present in HA ceramics,[30] and pyro- and piezoelectricity observed recently in hydroxyapatite thin films on silicon.[31]

4. Conclusions

DFT simulations and Rietveld refinement of the Sr-doped hydroxyapatite crystal have been carried out in the range of 0–100 at%, with the simulations considering the following sequences of substitution: (i) preferential substitution of Sr at Site II, (ii) preferential substitution of Sr at Site I, and (iii) mixed substitution. The structures were fully optimised allowing for changes in the HA unit cell volume and shape. The unit cell parameters *a* and *b* did not expand uniformly with the Sr doping. Whereas it has been observed that the mixed doping and progressive substitution of Sr into Ca-II sites causes certain distortions of the unit cell. On the other hand the gradual doping into Ca-I sites results in smaller and uniform expansion of the *a* and *b* lattice constants. The observed smaller and undistorted expansion of the crystal lattice can be associated with the uniform shift of the PO_4 tetrahedra, surrounding the Ca-I site, towards neighbouring hydroxyl channels, allowing for better accommodation of bigger ions of Sr at the Ca-I site.

To determine the specific site preference in doping of calcium HA with strontium at finite temperature, the free energy of mixing has been calculated from *ab initio* derived excess energy and ideal entropy of mixing as a function of Sr content. Our free energy calculations indicate that given a high-temperature calcination step in a typical synthesis route, the most energetically preferred substitution pattern is mixed Ca-I and Ca-II substitution. For a low-temperature wet-chemical synthesis, the contribution of the entropy of mixing to the stabilisation of the system is smaller but still sufficient to neutralise the endothermic nature of Sr substitution. At a temperature of 90 °C the mixed arrangement is still slightly favourable, except 20 at%, where also Site II substitution is permitted. These results allow for a deeper understanding of the observed experimentally preference for Sr doping in Site II at 15 and 25 at% as reported recently by Terra *et al.*[15]

We have also investigated changes in stability and structure of 50% Sr–HA by simulating the Sr doping at all possible Site I/Site II ratios. The most stable energetically appeared the ideal mixture with the fractional occupancy ratio Sr2/Sr1 = 1, where two Sr atoms were located at Ca-I and three Sr at Ca-II sites. With this arrangement of Sr in the calcium sublattice, the PO_4 tetrahedra were more rotated and tilted compared to

other Sr2/Sr1 ratios, imposing a crystal symmetry lowering and loss of center of symmetry. Based on our simulations it could be envisaged that the theoretically predicted PO_4 rotation in Sr-doped HA can potentially enhance dielectric properties of apatite such as pyroelectricity and piezoelectricity.

Acknowledgements

A contribution from the Bilateral Socrates-Erasmus Exchange Programme between University of Limerick and University of Münster is kindly acknowledged. We also acknowledge SFI/Higher Education Authority funded Irish Centre for High Performance Computing for the generous provision of computing resources.

References

1 H. Oonishi, *Biomaterials*, 1991, **12**, 171–178.
2 J. C. Elliot, *Structure and Chemistry of the Apatites and Other Calcium Orthophosphates*, Elsevier, Amsterdam, The Netherlands, 1994.
3 P. J. Marie, *Osteoporosis Int*., 2005, **16**, S7–S10.
4 C. Capuccini, P. Torricelli, E. Boanini, M. Gazzano, R. Giardino and A. Bigi, *J. Biomed. Mater. Res., Part A*, 2009, **89**, 594–600.
5 E. Boanini, P. Torricelli, M. Fini and A. Bigi, *J. Mater. Sci.: Mater. Med*., 2011, **22**, 2079–2088.
6 F. Yang, D. Z. Yang, J. Tu, Q. X. Zheng, L. T. Cai and L. P. Wang, *Stem Cells*, 2011, **29**, 981–991.
7 S. L. Peng, X. S. Liu, G. Q. Zhou, Z. Y. Li, K. D. K. Luk, X. E. Guo and W. W. Lu, *J. Bone Miner. Res*., 2011, **26**, 1272–1282.
8 G. Romieu, X. Garric, S. Munier, M. Vert and P. Boudeville, *Acta Biomater*., 2010, **6**, 3208–3215.
9 E. Boanini, M. Gazzano and A. Bigi, *Acta Biomater*., 2010, **6**, 1882–1894.
10 K. Zhu, K. Yanagisawa, R. Shimanouchi, A. Onda and K. Kajiyoshi, *J. Eur. Ceram. Soc*., 2006, **26**, 509–513.
11 A. Bigi, E. Boanini, C. Capuccini and M. Gazzano, *Inorg. Chim. Acta*, 2007, **360**, 1009–1016.
12 Z. Y. Li, W. M. Lam, C. Yang, B. Xu, G. X. Ni, S. A. Abbah, K. M. C. Cheung, K. D. K. Luk and W. W. Lu, *Biomaterials*, 2007, **28**, 1452–1460.
13 M. D. O'Donnell, Y. Fredholm, A. de Rouffignac and R. G. Hill, *Acta Biomater*., 2008, **4**, 1455–1464.
14 G. Renaudin, P. Laquerrière, Y. Filinchuk, E. Jallot and J. M. Nedelec, *J. Mater. Chem*., 2008, **18**, 3593–3600.
15 J. Terra, E. R. Dourado, J.-G. Eon and D. E. Ellis, *Phys. Chem. Chem. Phys*., 2009, **11**, 568–577.
16 K. Matsunaga and H. Murata, *J. Phys. Chem. B*, 2009, **113**, 3584–3589.
17 X. Ma and D. E. Ellis, *Biomaterials*, 2008, **29**, 257–265.
18 K. Matsunaga, *J. Chem. Phys*., 2008, **128**, 245101–245110.
19 K. Sudarsanan and R. A. Young, *Acta Crystallogr., Sect. B: Struct. Crystallogr. Cryst. Chem*., 1969, **25**, 1534–1543.
20 G. Kresse and J. Hafner, *Phys. Rev. B: Condens. Matter*, 1993, **47**, 558–561.
21 G. Kresse and J. Furthmüller, *Comput. Mater. Sci*., 1996, **6**, 15–50.
22 G. Kresse and J. Furthmüller, *Phys. Rev. B: Condens. Matter*, 1996, **54**, 11169–11186.
23 P. E. Blöchl, *Phys. Rev. B: Condens. Matter*, 1994, **50**, 17953–17979.
24 D. Joubert and G. Kresse, *Phys. Rev. B: Condens. Matter Mater. Phys*., 1999, **59**, 1758–1775.
25 J. P. Perdew, in *Electron Structure of Solids '91*, ed. P. Ziesche and H. Eschrig, Akademie Verlag, Berlin, 1991.
26 K. Sudarsanan and R. A. Young, *Acta Crystallogr., Sect. B: Struct. Crystallogr. Cryst. Chem*., 1972, **28**, 3668–3670.
27 A. Nounah, J. Szilagyi and J. L. Lacout, *Ann. Chim. (Cachan, Fr.)*, 1990, **15**, 409–419.
28 S. Gomes, J. M. Nedelec, E. Jallot, D. Sheptyakov and G. Renaudin, *Chem. Mater*., 2011, **23**, 3072–3085.
29 D. Haverty, S. A. M. Tofail, K. T. Stanton and J. B. McMonagle, *Phys. Rev. B: Condens. Matter Mater. Phys*., 2005, **71**, 094103.
30 S. A. M. Tofail, C. Baldisserri, D. Haverty, J. B. McMonagle and J. Erhart, *J. Appl. Phys*., 2009, **106**, 106104.
31 S. B. Lang, S. A. M. Tofail, A. A. Gandhi, M. Gregor, C. Wolf-Brandstetter, J. Kost, S. Bauer and M. Krause, *Appl. Phys. Lett*., 2011, **98**, 123703.